Adaptive Beamforming via Desired Signal Robust Removal for Interference-Plus-Noise Covariance Matrix Reconstruction

Pan Zhang[1] · Zhiwei Yang[2] · Gang Jing[1] · Teng Ma[1]

Abstract

To tackle the problem of the desired signal (DS) steering vector mismatch, especially in the situation of direction-of-arrival error and array perturbations, a robust interference-plus-noise covariance matrix (INCM) reconstruction method based upon DS removal is presented. Unlike previous studies, this paper proposes to remove the DS component from the training data by building a blocking matrix, which is computed as the inverse of the DS-plus-noise covariance matrix (DSNCM). More specifically, to increase the robustness against arbitrary mismatches, the DS steering vector estimated as the prime eigenvector of the DS matrix, which is attained through integrating the Capon spectrum estimator over the annulus uncertainty sets of the mainlobe region in advance, is adopted to give a faithful blocking matrix. After that, utilizing the obtained blocking matrix to process the training data, the quasi INCM is computed indeed. Finally, a precise INCM is reconstructed by projecting the principal components of the quasi INCM onto the aforesaid DSNCM. Numerical simulations have illustrated that the proposed adaptive beamformer can outperform the existing ones and gain almost optimal performance under different scenarios.

✉ Pan Zhang
     zp1339@foxmail.com

     Zhiwei Yang
     yangzw@xidian.edu.cn

     Gang Jing
     jg_xian@163.com

     Teng Ma
     1219mateng@163.com

[1] Beijing Institute of Radio Measurement, Beijing 100854, China

[2] National Laboratory of Radar Signal Processing, Xidian University, Xi'an 710071, China

1 Introduction

As a basic implementation to achieve spatial filtering, adaptive beamforming has been applied to several areas, such as radar, sonar, remote sensing, seismology, wireless communication, etc. [17, 20, 21]. The classical standard Capon beamformer (SCB) [2], as a well-known adaptive beamformer, can perform well if the knowledge of the desired signal (DS) steering vector is accurately estimated. However, this beamformer will suffer from severe performance degradation in the presence of the DS component in the training data, which is called the signal self-nulling effect, when the DS steering vector mismatches its true value due to direction-of-arrival (DOA) error and array imperfections [12, 23]. Thus, the study for improving the robustness of the SCB becomes fairly important.

During past decades, numerous robust adaptive beamforming approaches have been developed [3–5, 7, 10, 13, 14, 22, 27, 29, 30]. For instance, the diagonal loading (DL) algorithm in [10] is known as a popular technique, which adds a fixed identity matrix to the sample covariance matrix (SCM). Although the DL has been further studied in [4, 27] to decide a preferable loading factor, it is incapable of reducing the steering vector of the DS mismatch. To deal with this problem, the eigenspace-based beamformer (ESB) in [5] directly projects the DS steering vector onto the signal-plus-interference subspace to alleviate the mismatch. But the subspace swap happened at low signal-to-noise ratio (SNR) case leads to the increased steering vector of the DS mismatch. Considering the shortages in the aforementioned approaches, the robust Capon beamformer (RCB) in [22] estimates the steering vector of the DS by maximizing the output power in a user-defined uncertainty set. Note that the limited performance improvement on the RCB can be ascribed to the insufficient constraint on the steering vector of the DS.

As we all know, the presence of the signal self-nulling effect at high SNR case can be attributed to the DS-involved SCM or training data. In other words, estimating the INCM [6, 8, 11, 18, 25, 28, 31–33] or DS-free data [1, 9, 15, 16, 19, 24] has the potential to significantly improve the robustness of the SCB. Under this condition, the INCM-quadratically constrained quadratically programming (INCM-QCQP) algorithm in [6] reconstructs the INCM with the Capon spectrum estimator in the spatial region outside the DS region, which can attain good performance in the situation of well-calibrated array. To continue, the annulus uncertainty sets-INCM (AUS-INCM) reconstruction way in [8] employs the surface integral instead of the curve integral used in [6] to estimate the INCM with the Capon spectrum estimator in the interference regions. Nonetheless, this approach suffers from a large amount of high dimension calculations. In [25], a novel subspace-based INCM (NS-INCM) estimation method provides to pre-estimate the interference steering vectors with the Capon spectrum estimator in the known small spatial regions, then utilize the projection technique to yield the enhanced ones. This method improves the accuracy on estimating the interference steering vectors but still fails to reject the interferences completely at defective array structure case. Motivated by the unsettled issues above, the middle subarray-based

INCM estimation (MSB-INCM) method in [11] proposes to establish a selection matrix to transform the training data with mutual coupling into the middle subarray training data without mutual coupling, and then combine the idea in the INCM-QCQP to reconstruct the INCM. However, the MSB-INCM is not suitable for other common scenarios such as the channel gain and phase uncertainties and sensor position displacements. Different from the aforementioned INCM direct estimation algorithms, the multiple constrained L-2-norm minimization method in [15] removes the DS component from the SCM via building a blocking matrix with the presumed DS steering vector and a power adjust factor with small magnitude. Even though this algorithm is computationally efficient, its DS blocking capability at high DS power level case is unsatisfactory, which leads to the reduced output SINR.

In this paper, an INCM reconstruction method is devised through separating the DS component from the training data with a blocking matrix, where the blocking matrix is formed with the major eigenvector related to the Capon spectrum integral-based DS matrix. Then, the quasi INCM is calculated using the DS-absent data we obtained. At last, the dominant eigenvectors of the quasi INCM are processed by the inverse of the blocking matrix, which leads to the INCM reconstruction.

The paper contributes to the field of adaptive beamforming in the following aspects,

1. We propose a low-complexity INCM reconstruction algorithm using blocking matrix construction and matrix transition, which is manifestly different from the existing INCM direct estimation-based beamformers.
2. We provide a novel steering vector of the DS estimation method through applying eigendecomposition on the reconstructed DS matrix, which is obtained by integrating the Capon spectrum estimator over the annulus uncertainty sets of the possible DS region.
3. We give the performance comparisons of the proposed and relevant beamformers using typical experiments. Apparently, the proposed robust beamforming method can not only tackle the signal self-nulling effect but also preserve desired anti-interference capacity in the situation of DOA error and array perturbations.

The rest of this paper is organized as follows. In Sect. 2, the problem is formulated. In Sect. 3, the proposed method is introduced in detail. Section 4 contains several simulations. Conclusions are given in Sect. 5.

2 Problem Formulation

Consider a linear array with M sensors, receiving far-field narrowband signals including one DS and J interferences. The array sample data at the kth snapshot is modeled as:

$$\mathbf{x}(k) = \mathbf{a}_0 s_0(k) + \sum_{i=1}^{J} \mathbf{a}_i s_i(k) + \mathbf{n}(k) \qquad (1)$$

where $\mathbf{a}_i, i = 0, 1, \ldots, J$ and $s_i(k), i = 0, 1, \ldots, J$ represent the steering vector and waveform of the ith source, respectively, $\mathbf{n}(k)$ is Gaussian white noise. Here, the DS, interferences, and noise are assumed to be statistically independent at each snapshot. Then, the covariance matrix can be written as:

$$\mathbf{R} = E\{\mathbf{x}(k)\mathbf{x}^{\mathrm{H}}(k)\} = \mathbf{R}_s + \mathbf{R}_{\mathrm{in}} \qquad (2)$$

where $E\{\cdot\}$ and $(\cdot)^{\mathrm{H}}$ denote the statistical expectation and conjugate transpose, respectively, $\mathbf{R}_s$ and $\mathbf{R}_{\mathrm{in}}$ denote the ideal DS matrix and INCM, respectively.

Given a weight vector $\mathbf{w}$, the output SINR is always defined as:

$$\mathrm{SINR} = \frac{w^{\mathrm{H}}R_s w}{w^{\mathrm{H}}R_{\mathrm{in}} w} = \frac{\sigma_0^2 |w^{\mathrm{H}}\mathbf{a}_0|^2}{w^{\mathrm{H}}R_{\mathrm{in}} w} \qquad (3)$$

To reach the maximum output SINR, the SCB intends to minimize the array output power with a fixed and undistorted response constraint on the steering vector of the DS. The corresponding problem of the SCB is formulated as:

$$\min_{\mathbf{w}} \mathbf{w}^{\mathrm{H}}\mathbf{R}\mathbf{w} \text{ s.t. } \mathbf{w}^{\mathrm{H}}\mathbf{a}_0 = 1 \qquad (4)$$

with the solution $\mathbf{w}_{\mathrm{scb}} = \mathbf{R}^{-1}\mathbf{a}_0/\mathbf{a}_0^{\mathrm{H}}\mathbf{R}^{-1}\mathbf{a}_0$.

Since the theoretical covariance matrix $\mathbf{R}$ is unavailable, it is always replaced by its maximum likelihood estimate (i.e., the SCM), that is:

$$\hat{\mathbf{R}} = \frac{1}{K} \sum_{k=1}^{K} \mathbf{x}(k)\mathbf{x}^{\mathrm{H}}(k) \qquad (5)$$

where K denotes the number of snapshots.

As stated earlier, if the actual steering vector of the DS $\mathbf{a}_0$ is not precisely given, the performance of the SCB will severely drop, particularly at high SNR case, which can be attributed to the DS-contained SCM $\hat{\mathbf{R}}$.

To eliminate the DS component from the SCM $\hat{\mathbf{R}}$, Gu et al. have provided to reconstruct the INCM as [6]:

$$\breve{\mathbf{R}}_{\mathrm{in}} = \int_{\bar{\Theta}_s} \frac{\mathbf{a}(\theta)\mathbf{a}^{\mathrm{H}}(\theta)}{\mathbf{a}^{\mathrm{H}}(\theta)\hat{\mathbf{R}}^{-1}\mathbf{a}(\theta)}\mathrm{d}\theta \qquad (6)$$

where $\bar{\Theta}_s$ denotes the complementary region of the DS region, and $\mathbf{a}(\theta)$ stands for the steering vector of θ. Inevitably, the INCM reconstructed as above cannot involve actual interference component when the array is uncalibrated.

In terms of the shortcoming in (6), Huang et al. have offered to estimate the INCM as [8]:

$$\bar{\mathbf{R}}_{\text{in}} = \frac{1}{2} \int\limits_{\varTheta_{\text{int}}} \int\limits_{S_{\text{int}}} \frac{\tilde{\mathbf{a}}(\theta)\tilde{\mathbf{a}}^{\text{H}}(\theta)}{\tilde{\mathbf{a}}^{\text{H}}(\theta)\hat{\mathbf{R}}^{-1}\tilde{\mathbf{a}}(\theta)} \mathrm{d}\sigma \mathrm{d}\theta + \tilde{\sigma}_n^2 \mathbf{I} \tag{7}$$

where $\bar{\varTheta}_{\text{int}}$, $\tilde{\mathbf{a}}(\theta)$, $S_{\text{int}} = \{\,\tilde{\mathbf{a}}(\theta) |\; ||\tilde{\mathbf{a}}(\theta) - \mathbf{a}(\theta)|| = \varepsilon\,\}$, and $\tilde{\sigma}_n^2 \mathbf{I}$ are the interference region, steering vector located in the surface S_{int}, surface of the uncertainty set ε corresponding to the steering vector $\mathbf{a}(\theta)$, and noise matrix with power estimation $\tilde{\sigma}_n^2$, respectively. $||\cdot||$ represents the L-2 norm and $\mathbf{I}$ denotes the identity matrix. Undoubtedly, this INCM estimation scheme costs high complexity in covering the actual interference steering vectors, in view of that the region $\varTheta_{\text{int}}$ generally includes several interfering signals.

3 Proposed Algorithm

In this section, a reconstruction-based adaptive beamforming algorithm, which aims at simultaneously overcoming the signal self-nulling effect at high SNR case and preserving the anti-interference ability under array uncalibrated or partly calibrated environment, is proposed through constructing a blocking matrix to remove the DS component from the training data, then performing some concise matrix transitions to attain the INCM.

3.1 Blocking Matrix Construction

To construct the DS blocking matrix, the definition of the DS-plus-noise covariance matrix (DSNCM) is firstly given as:

$$\mathbf{R}_{\text{sn}} = \tilde{\sigma}_0^2 \mathbf{a}_0 \mathbf{a}_0^{\text{H}} + \tilde{\sigma}_n^2 \mathbf{I} \tag{8}$$

where $\tilde{\sigma}_0^2$ denotes the pre-defined DS power. Therefore, the DSNCM $\mathbf{R}_{\text{sn}}$ can be eigendecomposed as:

$$\mathbf{R}_{\text{sn}} = \sum_{i=1}^{M} \mu_i \mathbf{p}_i \mathbf{p}_i^{\text{H}} \tag{9}$$

where $\mu_i, i = 1, 2, \ldots, M$ denote the eigenvalues in descending order, while $\mathbf{p}_i$ are the corresponding eigenvectors. Subsequently, the inverse of the DSNCM can be expressed as follows if the pre-defined DS power is relatively higher than that of the noise (i.e., $\tilde{\sigma}_0^2 \gg \tilde{\sigma}_n^2$):

$$\mathbf{R}_{\text{sn}}^{-1} = \sum_{i=1}^{M} \frac{\mathbf{p}_i \mathbf{p}_i^{\text{H}}}{\mu_i} = \frac{\mathbf{p}_1 \mathbf{p}_1^{\text{H}}}{M\tilde{\sigma}_0^2 + \tilde{\sigma}_n^2} + \sum_{i=2}^{M} \frac{\mathbf{p}_i \mathbf{p}_i^{\text{H}}}{\tilde{\sigma}_n^2} \tag{10}$$

In view of that the conditions $\tilde{\sigma}_0^2 \gg \tilde{\sigma}_n^2$ and $\sum_{i=1}^{M} \mathbf{p}_i \mathbf{p}_i^{\text{H}} = \mathbf{I}$ are fulfilled, the inverse of the DSNCM $\mathbf{R}_{\text{sn}}^{-1}$ can be further approximated as:

$$\mathbf{R}_{\mathrm{sn}}^{-1} \cong \sum_{i=2}^{M} \frac{\mathbf{p}_i \mathbf{p}_i^{\mathrm{H}}}{\tilde{\sigma}_n^2} = \frac{\mathbf{I} - \mathbf{p}_1 \mathbf{p}_1^{\mathrm{H}}}{\tilde{\sigma}_n^2} \tag{11}$$

Hence, we can construct the blocking matrix as:

$$\mathbf{B} = \mathbf{R}_{\mathrm{sn}}^{-1} \tag{12}$$

where the blocking matrix $\mathbf{B}$ currently performs the feature $\mathbf{Ba}_0 \cong \mathbf{0}$ with $\mathbf{0}$ being the all-zero column vector.

To confirm the performance of the blocking matrix $\mathbf{B}$ with considering the DS power $\tilde{\sigma}_0^2$ selection problem, the function $||\mathbf{Ba}(\theta)||$ versus DOA under different DS power settings $\tilde{\sigma}_0^2 \in \{10\tilde{\sigma}_n^2, 10^2\tilde{\sigma}_n^2, 10^3\tilde{\sigma}_n^2, 10^2 trace(\hat{\mathbf{R}})\}$ is plotted in Fig. 1, where $trace(\cdot)$ stands for the trace of a matrix. In this example, the simulation parameters in Sect. 4 are used. As we can see from Fig. 1, if the DS power satisfies $\tilde{\sigma}_0^2 > 10^2\tilde{\sigma}_n^2$, the performance of the blocking matrix $\mathbf{B}$ seems unchanged and nearly excellent, which means that the qualification $\tilde{\sigma}_0^2 \gg \tilde{\sigma}_n^2$ is now met. Remarking that, on account of that the SCM $\hat{\mathbf{R}}$ always contains strong interferences and $trace(\hat{\mathbf{R}}) > \tilde{\sigma}_n^2$ is tenable, we have $10^2 trace(\hat{\mathbf{R}}) \gg \tilde{\sigma}_n^2$. Therefore, for general cases, a reasonable choice of the pre-defined power of the DS is given as $\tilde{\sigma}_0^2 = 10^2 trace(\hat{\mathbf{R}})$.

3.2 Interference-Plus-Noise Covariance Matrix Reconstruction

Based on the discussions above, the blocking matrix $\mathbf{B}$ is herein utilized to process the training samples $\mathbf{x}(k)$ as:
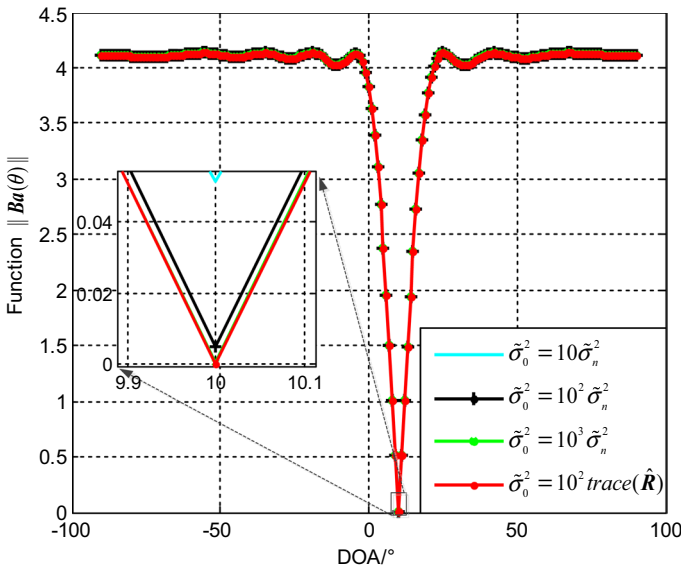

Fig. 1 Function $||\mathbf{Ba}(\theta)||$ versus DOA in the scenario of exactly known DS steering vector, $K = 80$ and SNR $= 15$ dB

$$\tilde{\mathbf{x}}(k) = \mathbf{B}\mathbf{x}(k) = \mathbf{B}\mathbf{a}_0 s_0(k) + \sum_{i=1}^{J} \mathbf{B}\mathbf{a}_i s_i(k) + \mathbf{B}\mathbf{n}(k) \tag{13}$$

It should be pointed out that the DS component $\mathbf{a}_0 s_0(k)$ has been blocked or significantly weakened in (13), and then, the term $\mathbf{B}\mathbf{a}_0 s_0(k)$ can be omitted, which follows the equivalent form of (13) as:

$$\tilde{\mathbf{x}}(k) \cong \sum_{i=1}^{J} \mathbf{B}\mathbf{a}_i s_i(k) + \mathbf{B}\mathbf{n}(k) \tag{14}$$

Accordingly, the covariance matrix, which is termed as the quasi INCM, can be computed as:

$$\tilde{\mathbf{R}}_{\text{in}} = \frac{1}{K} \sum_{k=1}^{K} \tilde{\mathbf{x}}(k)\tilde{\mathbf{x}}^{H}(k) = \sum_{i=1}^{J} \sigma_i^2 \mathbf{B}\mathbf{a}_i \mathbf{a}_i^{H} \mathbf{B}^{H} + \sigma_n^2 \mathbf{B}\mathbf{B}^{H} \tag{15}$$

Considering that the noise component in (15) has not been the ideal white one (i.e. $\sigma_n^2 \mathbf{I}$), the quasi INCM $\tilde{\mathbf{R}}_{\text{in}}$ needs to be modified as:

$$\widehat{\mathbf{R}}_{\text{in}} = \tilde{\mathbf{R}}_{\text{in}} - \tilde{\sigma}_n^2 \mathbf{B}\mathbf{B}^{H} + \tilde{\sigma}_n^2 \mathbf{I} \tag{16}$$

Subsequently, the quasi INCM after modification $\widehat{\mathbf{R}}_{\text{in}}$ can be eigendecomposed as:

$$\widehat{\mathbf{R}}_{\text{in}} = \sum_{i=1}^{M} \lambda_i \mathbf{v}_i \mathbf{v}_i^{H} = \sum_{i=1}^{J} \mathbf{v}_i(\lambda_i - \tilde{\sigma}_n^2)\mathbf{v}_i^{H} + \tilde{\sigma}_n^2 \mathbf{I} \tag{17}$$

where $\lambda_i, i = 1, 2, \ldots, M$ denote the eigenvalues in descending order and $\mathbf{v}_i$ stand for the related eigenvectors. Since the modified quasi INCM $\widehat{\mathbf{R}}_{\text{in}}$ can also be represented as:

$$\widehat{\mathbf{R}}_{\text{in}} = \sum_{i=1}^{J} \sigma_i^2 \mathbf{B}\mathbf{a}_i \mathbf{a}_i^{H} \mathbf{B}^{H} + \tilde{\sigma}_n^2 \mathbf{I} \tag{18}$$

we can simply draw the following conclusion according to the equivalence between (17) and (18):

$$\sum_{i=1}^{J} \sigma_i^2 \mathbf{B}\mathbf{a}_i \mathbf{a}_i^{H} \mathbf{B}^{H} = \sum_{i=1}^{J} \mathbf{v}_i(\lambda_i - \tilde{\sigma}_n^2)\mathbf{v}_i^{H} \tag{19}$$

Obviously, if we left-multiply and right-multiply both sides of (19) by the inverse of the blocking matrix $\mathbf{B}^{-1}$ (i.e., the DSNCM $\mathbf{R}_{\text{sn}}$) and the inverse of the conjugate transpose of the blocking matrix $(\mathbf{B}^{H})^{-1}$, the exact interference component is recovered, which leads to the INCM reconstruction as:

$$\hat{\mathbf{R}}_{\text{in}} = \sum_{i=1}^{J} \mathbf{B}^{-1}\mathbf{v}_i(\lambda_i - \tilde{\sigma}_n^2)\mathbf{v}_i^{\text{H}}(\mathbf{B}^{\text{H}})^{-1} + \tilde{\sigma}_n^2\mathbf{I} \tag{20}$$

It is worth stressing that the proposed DS removal-based algorithm is significantly distinct from that in [19], which is based on the subarray-level processes and shrinks the DOFs of array. In addition, the robust beamformer in [15] cannot offer satisfactory DS blocking performance as ours when the input SNR level is high.

3.3 Steering Vector of the Desired Signal Estimation

Starting from the point that the actual steering vector of the DS $\mathbf{a}_0$ employed in (8) is always hard to be known, we prepare to estimate the steering vector of the DS in this subsection.

On the basis of the prior knowledge of the DS region Θ_s, the DS matrix can be gained by integrating the Capon spectrum estimator over the annulus uncertainty sets as:

$$\tilde{\mathbf{R}}_s = \frac{1}{2} \int\limits_{\Theta_s} \int\limits_{S_s} \frac{\tilde{\mathbf{a}}(\theta)\tilde{\mathbf{a}}^{\text{H}}(\theta)}{\tilde{\mathbf{a}}^{\text{H}}(\theta)\hat{\mathbf{R}}^{-1}\tilde{\mathbf{a}}(\theta)} \, \mathrm{d}\sigma \mathrm{d}\theta \tag{21}$$

where $S_s = \{\tilde{\mathbf{a}}(\theta)|\|\tilde{\mathbf{a}}(\theta) - \mathbf{a}(\theta)\| = \varepsilon\}$ stands for the surface of the uncertainty set ε corresponding to the steering vector $\mathbf{a}(\theta)$, and the constant factor 1/2 is used to avoid repetitive calculations.

It should be mentioned that at the special uncertainty set case $\varepsilon = 0$, the estimate of the DS matrix $\tilde{\mathbf{R}}_s$ in (21) is actually the preceding approach in [26]. Even though the principle of (21) is similar to that in [8], they still hold significant distinctions. The annulus uncertainty set-based Capon spectrum integration in [8] aims to obtain the accurate INCM, while the goal of (21) is to resolve the exact estimation on the DS steering vector.

The integration in (21) does not have closed form solution, so we have to replace it with the summation approximately as:

$$\tilde{\mathbf{R}}_s = \frac{1}{2} \sum_{i=1}^{I} \sum_{l=1}^{L} \frac{\mathbf{a}_l(\theta_i)\mathbf{a}_l^{\text{H}}(\theta_i)}{\mathbf{a}_l^{\text{H}}(\theta_i)\hat{\mathbf{R}}^{-1}\mathbf{a}_l(\theta_i)} \tag{22}$$

where $\mathbf{a}_l(\theta_i)$ denotes the lth steering vector at the ith grid in the DS angular region Θ_s, I and L represent the number of grids in the DS angular region Θ_s and the number of steering vectors for one grid, respectively.

Via the well-estimated DS matrix $\tilde{\mathbf{R}}_s$ in (22), the steering vector of the DS can be easily estimated as:

$$\tilde{\mathbf{a}}_0 = \sqrt{M}\frac{P\{\tilde{\mathbf{R}}_s\}}{\|P\{\tilde{\mathbf{R}}_s\}\|} \tag{23}$$

where $P\{\cdot\}$ represents the operation which returns the principal eigenvector of a matrix.

3.4 Weight Vector Calculation

Combining the steering vector of the DS $\tilde{\mathbf{a}}_0$ and INCM $\hat{\mathbf{R}}_{\mathrm{in}}$, the beamforming weight vector is acquired as:

$$\mathbf{w}_{\mathrm{pro}} = \frac{\hat{\mathbf{R}}_{\mathrm{in}}^{-1}\tilde{\mathbf{a}}_0}{\tilde{\mathbf{a}}_0^{\mathrm{H}}\hat{\mathbf{R}}_{\mathrm{in}}^{-1}\tilde{\mathbf{a}}_0} \tag{24}$$

Above all, the steps of the proposed DS robust removal-based INCM reconstruction algorithm, which is referred to as the DSRR-INCM, are summarized in Table 1. We can find that the computation load of the proposed algorithm mainly lies in estimating the steering vector of the DS and INCM. The computation loads of estimating the steering vector of the DS and INCM are $O((IL+K)M^2)+O(3\,M^3)$ and $O((K+J+2)M^2)+O((3+2\,J)M^3)$, respectively. As a result, the overall computation load of the proposed method is $O((IL+2\,K+J)M^2)+O((6+2\,J)M^3)$.

4 Simulation

A uniform linear array (ULA) with $M=8$ isotropic sensors spaced half wavelength apart is assumed. There are one DS and two interferences impinge on the ULA from $10°$, $-25°$, and $45°$, respectively. The interference-to-noise ratios (INR) of two strong interferences are 20 dB and the presumed DOA of the DS is $7°$.

To implement the proposed algorithm, the DS region Θ_s is set as $[2°, 12°]$, of which the number of grids I is fixed to 100. The DS power $\tilde{\sigma}_0^2 = 10^2 trace(\hat{\mathbf{R}})$ is fixed, and the noise power $\tilde{\sigma}_n^2$ is selected as the minimum eigenvalue of the SCM. Besides, for each $\theta_i \in \Theta_s$, the steering vector $\mathbf{a}_l(\theta_i)$ is determined as:

$$\mathbf{a}_l(\theta_i) = \mathbf{a}(\theta_i) + \frac{\varepsilon}{\sqrt{M}}[e^{j\phi_0^l}, e^{j\phi_1^l}, \cdots, e^{j\phi_{M-1}^l}] \tag{25}$$

where the uncertainty set $\varepsilon = \sqrt{0.1}$ and phases $\phi_i^l \in [0, 2\pi), i = 0, 1, \ldots, M - 1$ are selected, respectively. In order to sample at the surface S_s, we need to discretize the phases $\phi_i^l, i = 0, 1, \ldots, M - 1$ from 0 to 2π. As is acknowledged in [8], the number

Table 1 Steps of the proposed algorithm

1: Calculate the sample covariance matrix $\hat{\mathbf{R}}$ with (5)
2: Estimate the steering vector of the DS $\tilde{\mathbf{a}}_0$ with (22) and (23)
3: Construct the blocking matrix $\mathbf{B}$ with (8) and (12) by replacing $\mathbf{a}_0$ with $\tilde{\mathbf{a}}_0$
4: Reconstruct the INCM $\hat{\mathbf{R}}_{\mathrm{in}}$ with (13), (15)–(17), and (20)
5: Obtain the adaptive weight vector $\mathbf{w}_{\mathrm{pro}}$ with (24)

of discrete values in $[0, 2\pi)$ should be greater than or equal to two, so we uniformly choose two values in $[0, 2\pi)$ as the sample points of the phases $\phi_i^l, i = 0, 1, \ldots, M - 1$ (i.e. $\phi_i^l, i = 0, 1, \ldots, M - 1$ equals to 0 or π), which means that the number of steering vectors for one grid $L = M^2$ is fixed.

For comparison purpose, the performance of the DL [10], ESB [5], RCB [22], INCM-QCQP [6], AUS-INCM [8], NS-INCM [25], and MCLM [15] is tested as well. The loading factor in the DL is set as $10\tilde{\sigma}_n^2$. The upper norm bound in the RCB is taken as 0.3 M. In addition, the complementary region of the DS region $\bar{\Theta}_s$ in the INCM-QCQP is chosen as $[-90°, 2°)\cup(12°, 90°]$, of which the number of grids is fixed to 500. Moreover, for the AUS-INCM, the interference region Θ_{int} is selected as $[-27°, -17°]\cup[37°, 47°]$, of which the numbers of grids is fixed to 200, the uncertainty set and sample points in the surface around the steering vector located in the region of the interferences are set the same as that in the DSRR-INCM. The region of incoming signals in the NS-INCM is $[2°, 12°]\cup[-27°, -17°]\cup[37°, 47°]$, of which the number of grids is fixed to 300. The power adjustment factor in the MCLM is selected as $\min\{0.02, M/\text{trace}(\hat{\mathbf{R}})\}$. The optimal SINR (OPT) is calculated as $\text{SINR}_{\text{opt}} = \sigma_0^2 \mathbf{a}_0^H \mathbf{R}_{\text{in}}^{-1} \mathbf{a}_0$ with σ_0^2 being the true power of the DS. Each result in this section is an average of 300 Monte-Carlo simulations.

4.1 Performance Under Different DS Power Pre-definitions

In this subsection, we explore the influence of different DS power pre-definitions, i.e., $\tilde{\sigma}_0^2 \in \{10\tilde{\sigma}_n^2, 10^2\tilde{\sigma}_n^2, 10^3\tilde{\sigma}_n^2, 10^2\text{trace}(\hat{\mathbf{R}})\}$, on the output performance
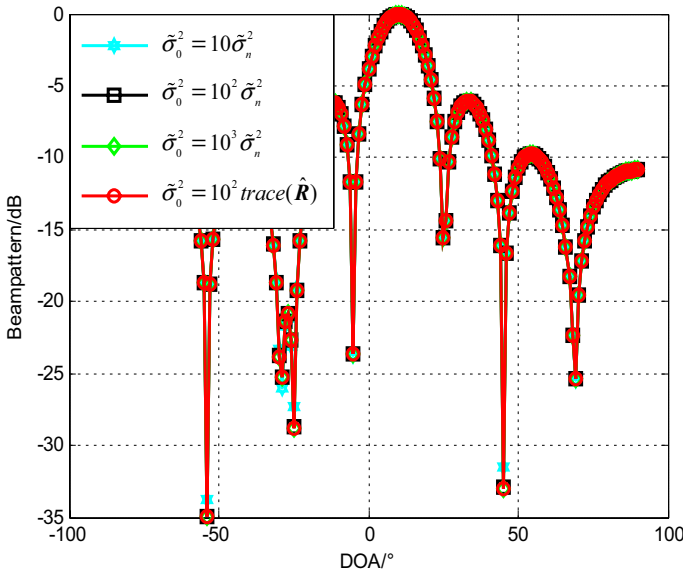

Fig. 2 Beampattern versus DOA in the scenario of exactly known DS steering vector, SNR = 15 dB and $K = 80$
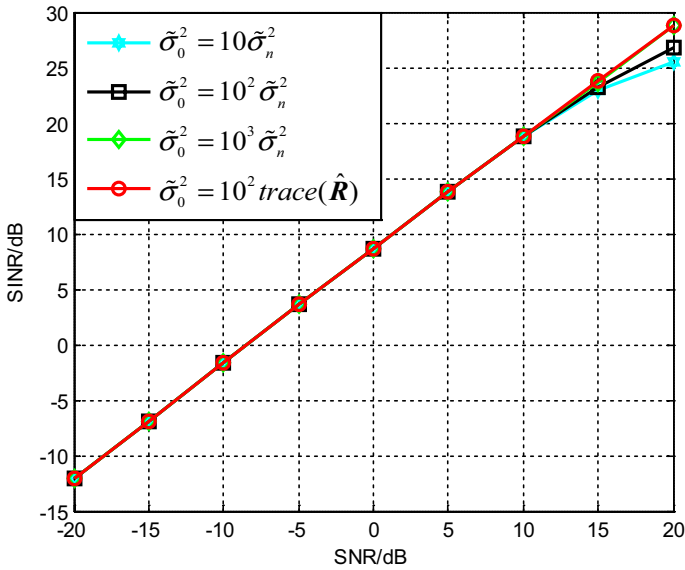
Fig. 3 SINR versus SNR in the scenario of exactly known DS steering vector, $K = 80$

of the DSRR-INCM. Figures 2 and 3 exhibit the beampattern versus DOA and output SINR versus input SNR, respectively. It is observed that in Fig. 2, if and only if $\tilde{\sigma}_0^2 = 10^3 \tilde{\sigma}_n^2$ and $\tilde{\sigma}_0^2 = 10^2 trace(\hat{\mathbf{R}})$ are utilized, the proposed DSRR-INCM has desired and stable beampattern with deeper nulls than others and thus owns great interference rejection ability. In line with the consequence in Fig. 2, we can view from Fig. 3 that the DSRR-INCM with pre-defined DS powers $\tilde{\sigma}_0^2 = 10^3 \tilde{\sigma}_n^2$ and $\tilde{\sigma}_0^2 = 10^2 trace(\hat{\mathbf{R}})$ performs best among other DS power settings. That is, the offered algorithm can hold excellent performance for large dynamic SNR changing scenarios when $\tilde{\sigma}_0^2 > 10^2 \tilde{\sigma}_n^2$ is satisfied. Noting that, on account of that the SCM permanently comprises strong interferences and $trace(\hat{\mathbf{R}}) > \tilde{\sigma}_n^2$ is tenable, the pre-defined DS power can be directly set as $\tilde{\sigma}_0^2 = 10^2 trace(\hat{\mathbf{R}})$ to make the proposed beamformer applicable for general cases.

4.2 Mismatch Due to DOA Error

In this example, the DOA error is just considered. Figure 4 shows the average SINR of different approaches against SNR. It is apparent that the INCM reconstruction-based methods, including the INCM-QCQP, AUS-INCM, NS-INCM, and DSRR-INCM, can achieve almost idea performance at both low and high SNR cases due to the effective estimate of the INCM. However, the ESB and RCB cannot work well at high SNR case because of the signal self-nulling effect. Although the MCLM can maintain mainbeam, the reduced anti-interference performance resulted from the unsatisfactory DS elimination still leads to output
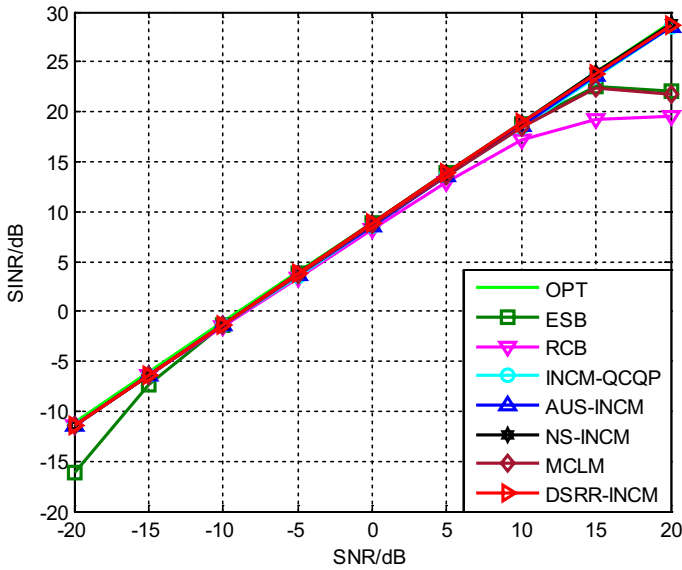
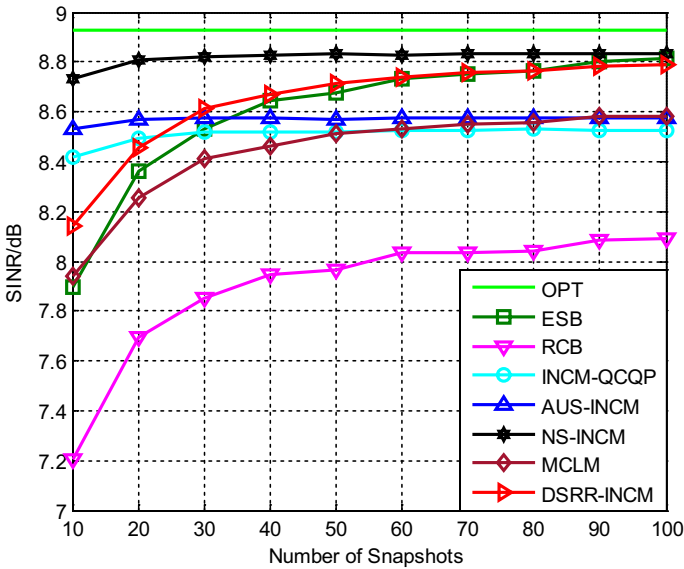**Fig. 4** SINR versus SNR in the scenario of DOA error, $K = 80$

Fig. 5 SINR versus number of snapshots in the scenario of DOA error, SNR = 0 dB

SINR loss. Moreover, the SINR versus number of snapshots is depicted in Fig. 5. Again, the proposed DSRR-INCM can offer desired output SINR in the situation of small training samples.

4.3 Mismatch Due to DOA and Sensor Position Errors

The third example is carried out under both DOA and sensor position errors, where each sensor is set to be far away from its theoretical position, to obey uniform distribution of [−0.05, 0.05] measured in wavelength. Following the second example, the SINR versus SNR is exhibited in Fig. 6. Obviously, the DSRR-INCM outperforms other compared approaches, which can be owing to the DS blocking-based INCM reconstruction procedure and uncertainty set-based DS steering vector estimation. It should be mentioned that at SNR > 18 dB case, the small output SINR drop of the devised DSRR-INCM can be attributed to the insufficient samples in the annulus uncertainty sets in estimating the DS steering vector. Additionally, the SINR versus number of the snapshots is plotted in Fig. 7, we can observe that the proposed method shows enough robustness when number of snapshots is limited.

4.4 Mismatch Due to DOA and Gain and Phase Errors

The fourth example is executed in the scenario of DOA and sensor gain and phase errors, where the sensor gain error and phase error are subjected to the normal distributions in [−0.5 dB, 0.5 dB] and [−5°, 5°], respectively. Following the second and third examples, the SINR versus SNR and SINR versus number of snapshots are displayed in Figs. 8 and 9, respectively. Clearly, the ESB, RCB, MCLM, and INCM direct estimation methods, including the INCM-QCQP, AUS-INCM, and NS-INCM, cannot remain superior performance when SNR is high or size of training samples is finite as compared to the proposed algorithm, which can be ascribed
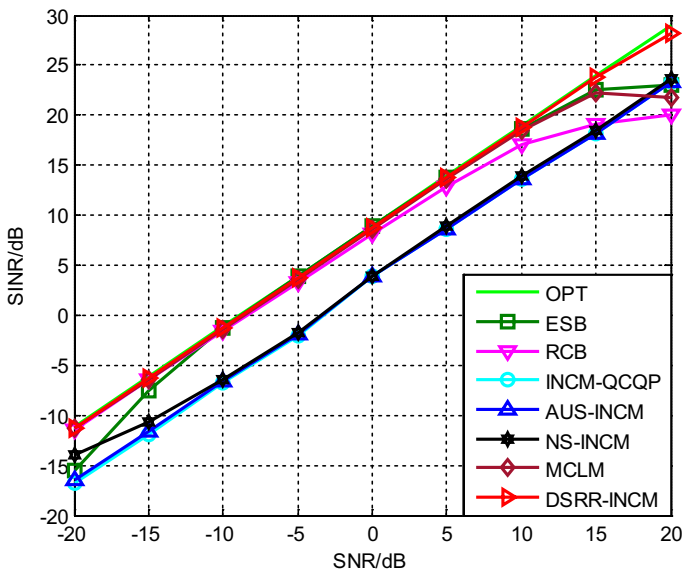

Fig. 6 SINR versus SNR in the scenario of DOA and sensor position errors, $K = 80$
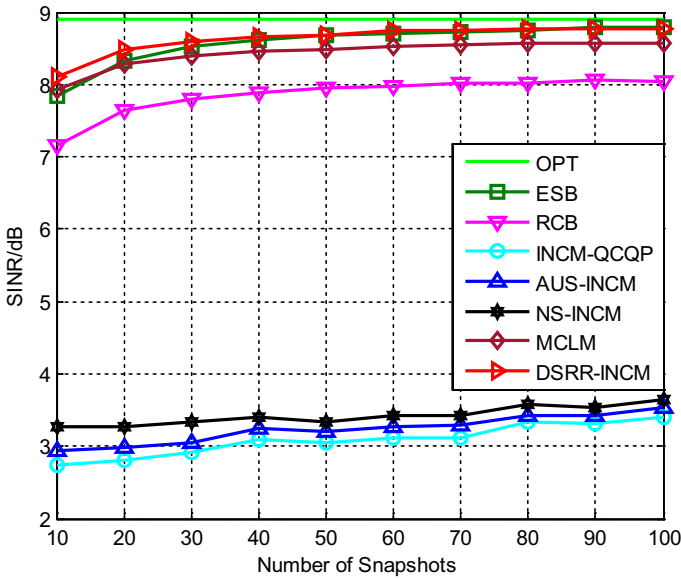
Fig. 7 SINR versus number of snapshots in the scenario of DOA and sensor position errors, SNR = 0 dB
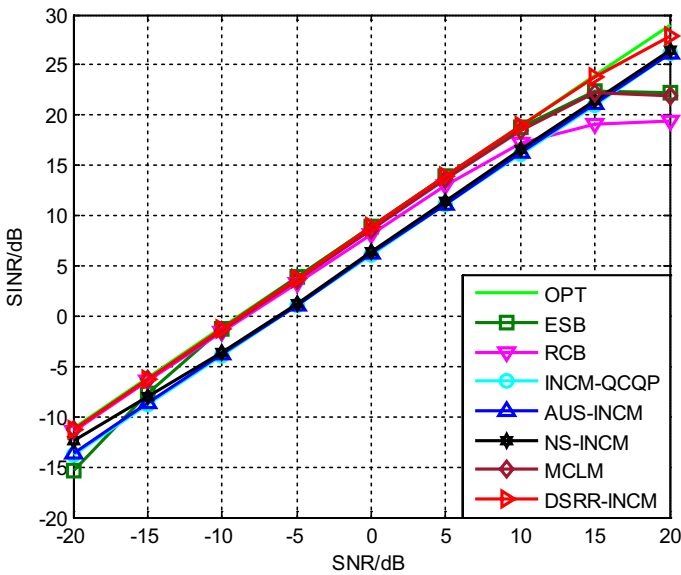

Fig. 8 SINR versus SNR in the scenario of DOA and sensor gain and phase errors, $K = 80$

to our novel DS removal-based INCM reconstruction design. However, due to the inaccurate estimate of the DS steering vector, the SINR reduction of the DSRR-INCM at SNR > 15 dB case should not be missed. Our future work will focus on
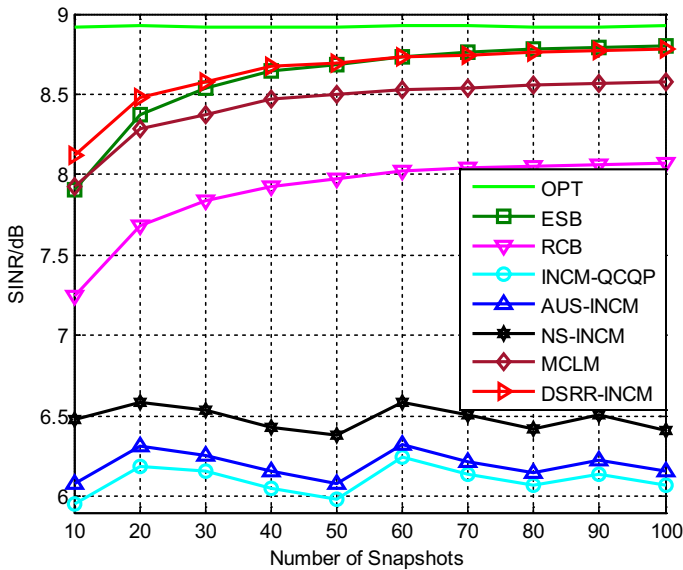
Fig. 9 SINR versus number of snapshots in the scenario of DOA and sensor gain and phase errors, SNR = 0 dB

improving the DS steering vector estimation accuracy, to further develop the proposed beamformer.

5 Conclusion

A DS robust removal-based INCM reconstruction method is introduced in this paper, whose main purpose is to combat the problem of the DS steering vector mismatch. Particularly, the steering vector of the DS is first estimated by realizing the DS matrix with the Capon spectrum estimator and annulus uncertainty set. Secondly, the construction of the blocking matrix is completed via the well-estimated DS steering vector and pre-defined power, which results in the estimate of the quasi INCM by processing the training samples with the blocking matrix. Finally, through projecting the prime eigenvectors related to the quasi INCM onto the inverse of the blocking matrix, the INCM reconstruction is achieved indeed. Representative experiments have validated the robustness improvement of the proposed method, especially when both DOA error and array imperfections exist and the training data contains the DS component.

Compliance with Ethical Standards

Conflict of interest The authors declare that they have no conflict of interests.

References

1. K.M. Buckley, L.J. Griffths, An adaptive generalized sidelobe canceller with derivative constraints. IEEE Trans. Antennas Propag. **34**(3), 311–319 (1986)
2. J. Capon, High-resolution frequency-wave number spectrum analysis. Proc. IEEE **57**(8), 1408–1418 (1969)
3. L. Chang, C.C. Yeh, Performance of DMI and eigenspace-based beamformers. IEEE Trans. Antennas Propag. **40**(11), 1336–1347 (1992)
4. L. Du, J. Li, P. Stoica, Fully automatic computation of diagonal loading levels for robust adaptive beamforming. IEEE Trans. Aerosp. Electron. Syst. **46**(1), 449–458 (2010)
5. D.D. Feldman, L.J. Griffiths, A projection approach for robust adaptive beamforming. IEEE Trans. Signal Process. **42**(4), 867–876 (1994)
6. Y.J. Gu, A. Leshem, Robust adaptive beamforming based on interference covariance matrix reconstruction and steering vector estimation. IEEE Trans. Signal Process. **60**(7), 3881–3885 (2012)
7. F. Huang, W. Sheng, X. Ma, Modified projection approach for robust adaptive array beamforming. Signal Process. **92**(7), 1758–1763 (2012)
8. L. Huang, J. Zhang, X. Xu, Z.F. Ye, Robust adaptive beamforming with a novel interference-plus-noise covariance matrix reconstruction method. IEEE Trans. Signal Process. **63**(7), 1643–1650 (2015)
9. N.K. Jablon, Adaptive beamforming with the generalized sidelobe canceller in the presence of array imperfections. IEEE Trans. Antennas Propag. **34**(8), 996–1012 (1986)
10. J. Li, P. Stoica, Z. Wang, On robust Capon beamforming and diagonal loading. IEEE Trans. Signal Process. **51**(7), 1702–1715 (2003)
11. Z.H. Li, Y.S. Zhang, Q.C. Ge, Y.D. Guo, Middle subarray interference covariance matrix reconstruction approach for robust adaptive beamforming with mutual coupling. IEEE Commun. Lett. **23**(4), 664–667 (2019)
12. B. Liao, S.C. Chan, K.M. Tsui, Recursive steering vector estimation and adaptive beamforming under uncertainties. IEEE Trans. Aerosp. Electron. Syst. **49**(1), 489–501 (2013)
13. B. Liao, C.T. Guo, L. Huang, Q. Li, H.S. So, Robust adaptive beamforming with precise main beam control. IEEE Trans. Aerosp. Electron. Syst. **53**(1), 345–356 (2017)
14. J.P. Lie, W. Ser, C.M.S. See, Adaptive uncertainty based iterative robust Capon beamformer using steering vector mismatch estimation. IEEE Trans. Signal Process. **59**(9), 4483–4488 (2011)
15. F.L. Liu, R.Y. Du, J. Wu, Q.P. Zhou, Z.X. Zhang, Y.J. Cheng, Multiple constrained l2-norm minimization algorithm for adaptive beamforming. IEEE Sens. J. **18**(15), 6311–6318 (2018)
16. K.W. Lo, Improving performance of real-symmetric adaptive array by signal blocking. IEEE Trans. Aerosp. Electron. Syst. **31**(2), 821–830 (1995)
17. S. Mohammadzadeh, S. Kukrer, Robust adaptive beamforming with improved interferences suppression and a new steering vector estimation based on spatial power spectrum. Circuits Syst. Signal Process. **38**, 4162–4179 (2019)
18. J.H. Qian, Z.S. He, T. Liu, N. Huang, Robust beamforming based on steering vector and covariance matrix estimation. Circuits Syst. Signal Process. **37**, 4665–4682 (2018)
19. M. Rahmani, M.H. Bastani, S. Shahraini, Two layers beamforming robust against direction-of-arrival mismatch. IET Signal Process. **8**(1), 49–58 (2014)
20. I.S. Reed, J.D. Mallett, L.E. Brennan, Rapid convergence rate in adaptive arrays. IEEE Trans. Aerosp. Electron. Syst. **10**(6), 853–863 (1974)
21. H. Ruan, R.C. de Lamare, Robust adaptive beamforming based on low-rank and cross-correlation techniques. IEEE Trans. Signal Process. **64**(15), 3919–3932 (2016)
22. P. Stoica, Z. Wang, J. Li, Robust Capon beamforming. IEEE Signal Process. Lett. **10**(6), 172–175 (2003)
23. S.A. Vorobyov, A.B. Gershman, Z.Q. Luo, Robust adaptive beamforming using worst-case performance optimization: a solution to the signal mismatch problem. IEEE Trans. Signal Process. **51**(2), 313–324 (2003)
24. X.P. Yang, Z.A. Zhang, T. Zeng, T. Long, T.K. Sarkar, Mainlobe interference suppression based on eigen-projection processing and covariance matrix reconstruction. IEEE Antennas Wirel. Propag. Lett. **13**, 1369–1372 (2014)
25. X.L. Yuan, L. Gan, Robust adaptive beamforming via a novel subspace method for interference covariance matrix reconstruction. Signal Process. **130**, 233–242 (2017)

26. X.L. Yuan, L. Gan, Robust algorithm against large look direction error for interference-plus-noise covariance matrix reconstruction. Eletron. Lett. **52**(6), 448–450 (2016)
27. M. Zhang, A. Zhang, Q. Yang, Robust adaptive beamforming based on conjugate gradient algorithms. IEEE Trans. Signal Process. **64**(22), 6046–6057 (2016)
28. Y.P. Zhang, Y.J. Lin, M.G. Gao, Robust adaptive beamforming based on the effectiveness of reconstruction. Signal Process. **120**, 572–579 (2016)
29. X.J. Zhang, Z.S. He, B. Liao, X.P. Zhang, Z.Y. Cheng, Y.X. Li, A2RC: an accurate array response control algorithm for pattern synthesis. IEEE Trans. Signal Process. **65**(7), 1810–1824 (2017)
30. X.J. Zhang, Z.S. He, B. Liao, X.P. Zhang, W.L. Peng, Robust quasi-adaptive beamforming against direction-of-arrival mismatch. IEEE Trans. Aerosp. Electron. Syst. **54**(3), 1197–1207 (2018)
31. Z.Y. Zhang, W. Liu, W. Leng, A.G. Wang, H.P. Shi, Interference-plus-noise covariance matrix reconstruction via spatial power spectrum sampling for robust adaptive beamforming. IEEE Signal Process. Lett. **23**(1), 121–125 (2016)
32. Z. Zheng, W.Q. Wang, H.C. So, Y. Liao, Robust adaptive beamforming using a novel signal power estimation algorithm. Digital Signal Process. **95**, 102574 (2019)
33. X.Y. Zhu, X. Xu, Z.F. Ye, Robust adaptive beamforming via subspace for interference covariance matrix reconstruction. Signal Process. **167**, 233–242 (2020)